Metabolism Clinical and Experimental 98 (2019) 16–26

Contents lists available at ScienceDirect

Metabolism Clinical and Experimental

journal homepage: www.metabolismjournal.com

Basic Science

The glycoprotein follistatin-like 1 promotes brown adipose thermogenesis

Dongliang Fang [a], Xinyi Shi [a], Tao Lu [a], Haibin Ruan [b], Yan Gao [a,*]

[a] Beijing Key Laboratory of Cancer Invasion and Metastasis Research, Department of Human Anatomy, School of Basic Medical Sciences, Capital Medical University, Beijing 100069, China
[b] Department of Integrative Biology and Physiology, University of Minnesota Medical School, Minneapolis, MN 55455, USA

ARTICLE INFO

Article history:
Received 15 February 2019
Accepted 21 May 2019

Keywords:
Brown adipose tissue
Adaptive thermogenesis
β3-adrenergic receptor
FSTL1
Protein glycosylation

ABSTRACT

Objectives: The thermogenic brown adipose tissue (BAT) has been proposed as a potential target to prevent or treat obesity and related metabolic diseases. BAT secretes adipokines to regulate the thermogenic program in an autocrine or paracrine manner. Follistatin-like 1 (FSTL1), a glycoprotein involved in adipogenesis and obesity, however, the function of FSTL1 in BAT thermogenesis and in the regulation of systemic energy homeostasis are not fully understood.

Methods: Whole-body ablation *Fstl1* heterozygous mice (*Fstl1*$^{+/-}$) and its littermates control were injected with CL316,243 to assess energy balance. A series of FSTL1 overexpression and knockdown experiments were carried out to evaluate its function in regulating thermogenic gene expression in brown adipocytes.

Results: FSTL1 expression was induced upon BAT activation during cold challenge or β3-adrenergic activation. FSTL1 haploinsufficiency in mice led to reduced thermogenic gene expression, impaired BAT recruitment, and decreased heat production. FSTL1 cell-autonomously promoted the β3-adrenergic signaling, which was required to upregulate PPARγ and UCP1 in brown adipocytes. Furthermore, only glycosylated FSTL1 could be secreted from brown adipocytes to induce the β3-adrenergic activation.

Conclusions: Our results suggest FSTL1 as a novel stimulator of the β-adrenergic signaling and BAT thermogenesis.

1. Introduction

Obesity develops from perturbations in overall calorie balance when energy intake chronically exceeds total body energy expenditure. While most current medications and surgery for obesity target calorie intake and absorption, increasing energy consumption is being considered an attractive alternative [1,2]. Brown adipose tissue (BAT) has a remarkable energy dissipating capacity and actively promotes triglyceride clearance, glucose disposal, and generation of heat for thermogenesis [3,4]. The thermogenic activity of BAT depends on its high mitochondrial content and uncoupling protein 1 (UCP1), which uncouples the mitochondrial proton gradient from ATP synthesis to generate heat [5,6].

Several key factors in regulating BAT function have been identified such as peroxisome proliferator-activated receptor γ (PPARγ), PPARγ cofactor-1α (PGC-1α), and PR domain containing 16 (PRDM16) [7–9]. PPARγ, forming a heterodimer with retinoid X receptor (RXR), activates *Ucp1* gene expression by binding to the peroxisome proliferator response element (PPRE) in the *Ucp1* promoter [10]. PGC-1α and PRDM16, as transcription cofactors, bind to PPARγ to activate brown fat-specific gene expression [11]. Cold exposure and β-adrenergic activation are two best-characterized ways to activate brown fat [12,13]. Upon cold challenge, sympathetic nerve fibers release norepinephrine (NE) onto β-adrenergic receptors (β-ARs) on brown adipocytes and then initiate a signaling cascade in which cyclic AMP-activated protein kinase A (PKA) phosphorylates and activates the p38 mitogen-activated protein kinase (MAPK) pathway. PKA-stimulated cAMP response element binding (CREB) and p38 MAPK-phosphorylated PGC-1α in turn support the maximal induction of thermogenic capacity of BAT [14]. Treatment of obese rodents with β3-selective agonists reduces fat stores and improves obesity-induced insulin resistance [15]. In humans, a β3-AR agonist can stimulate BAT thermogenesis; however, its clinical application is hindered by potential adverse side effects [16].

Recently, a series of studies focused on the interactions between the extracellular matrix (ECM) and the metabolic syndrome [17,18]. In addition to thermoregulation, BAT secretes adipokines, as known as batokines, to control systemic glucose and lipid metabolism [19,20]. These factors include peptides and nonpeptidic molecules that have autocrine, paracrine, and endocrine actions (e.g. Bone morphogenetic protein 8b (BMP8b), 12,13-diHOME et. al) [21]. Follistatin was found to promote adipocyte differentiation, browning, and energy metabolism [22,23]. The identification

* Corresponding author at: Department of Human Anatomy, School of Basic Medical Sciences, Capital Medical University, No. 10, Xitoutiao, Youanmenwai, Fengtai District, Beijing 100069, China.
E-mail address: gy1003@ccmu.edu.cn (Y. Gao).

https://doi.org/10.1016/j.metabol.2019.05.008

and characterization of novel batokines may provide opportunities for therapeutic interventions in metabolic diseases.

Follistatin-like 1 (FSTL1) is a glycoprotein belonging to the secreted protein acid and rich in cysteine (SPARC) family [24]. FSTL1 comprises a follistatin module, a Kazal-like domain, two EF-hand domains, and a von Willebrand factor type C domain [25]. There are three potential sites for N-glycosylation and two for O-glycosylation in the sequence of mouse FSTL1 [26], N-glycoproteome analysis on human blood plasma identified only one glycosylated form of FSTL1 in which two (Asp^{175} and Asp^{180}) of the three sites are used. The highest levels of *Fstl1* mRNA are found in heart, lung, and subcutaneous white adipose tissue, and it is a robust hallmark of preadipocyte to adipocyte conversion [27]. Serum levels of FSTL1 were found to be higher in overweight and obese subjects than in controls [28]. Nonetheless, it is unclear whether FSTL1 is involved in the regulation of BAT function. Here, we identify that FSTL1 is highly expressed and glycosylated in BAT and it promotes the thermogenic program during cold exposure or β3-AR activation by enhancing β3-adrenergic signaling.

2. Materials and methods

2.1. Animal studies

Fstl1$^{flox/+}$ mice of a mixed background (129Sv/C57BL/6J) were purchased from Model Animal Research Center of Nanjing University. To meet the requirements for metabolic study, we have backcrossed *Fstl1*$^{flox/+}$ mice to a C57BL/6 J genetic background for >10 generations. Because of all *Fstl1*$^{-/-}$ homozygous pups breathed irregularly and displayed a cyanotic skin color, then died shortly after birth. While *Fstl1*$^{+/-}$ heterozygous mice did not show any obvious physiological abnormalities, *Fstl1*$^{+/-}$ mice were used in this study. All animal experiments were performed in accordance with the Administration Regulations on Laboratory Animals of Beijing Municipality. All animals were maintained under 12 h/12 h light/dark cycle under constant conditions of room temperature (22 °C) and humidity with free access to food and water. For HFD feeding experiments, 6–8 weeks old male mice were fed with HFD (60 kcal%, Research Diets Inc. D12492) diets for up to 12 weeks. Mouse genotyping was performed using genomic DNA isolated from mouse tails. The primer set of *Fstl1* we used was: forward, 5′-TCCCACCTTCGCCTCTAACT-3′; reverse, 5′-GAACTCTGCGGCTGCTCTG-3′. Agarose gel electrophoresis showed fragments of either 560 bp or 350 bp, which were produced from the WT or the null allele, respectively (Fig. S.4A). The details were shown in our previously study [29].

2.2. Metabolic phenotyping assays

We used both cold exposure (CE) and β3-adrenergic receptor agonist to activate brown fat. For acute cold exposure, 8-week-old male mice were placed in a refrigerator (4 °C) for 8 h without food and water. For long term cold exposure, mice were placed for 72 h with food and water. Mice were injected with CL316,243 (C5976; Sigma) at 1 mg/kg when needed. The core body temperature was monitored using a rectal probe (Omron, Dalian, China). Body temperature of mice was measured every hour for a total of 8 times after CL316,243 injection or placing in the refrigerator. To exclude the influence of other tissues on thermogenesis, we did BAT removal operation. Detailed surgical procedures are described in the supplementary material.

Body weight of mice was monitored weekly by a digital precision scale (accuracy 0.1 g). Body composition (fat and lean mass) was assayed by an EchoMRI system. For energy metabolism analysis of mice after regular diet (RD) or high fat diet (HFD) feeding or CL316,243 injection, a total of 72 h of monitoring was conducted, and the data of the latter 48 h were taken for analysis. Energy expenditure measurements were made using a Comprehensive Lab Animal Monitoring System (Columbus Instruments). Mice were acclimated to the Comprehensive Lab Animal Monitoring System (CLAMS) for at least 24 h prior to acquisition of data. Oxygen consumption (VO_2) and carbon dioxide production (VCO_2) were measured every 27 min for calculation of the respiratory exchange ratio ($RER = VCO_2/VO_2$) and energy expenditure ($EE = 3.815 + [(1.232 \times RER) \times VO_2]$ in kCal/[kg × h]). Food and water intake were measured every 27 min using a precision scale and volumetric drinking monitor, respectively. Ambulatory activity was estimated by the number of infrared beams broken along the x axis of the metabolic cage.

2.3. Glucose tolerance test and insulin tolerance test

To determine glucose tolerance, 16-h-fasted mice were intraperitoneally administered with glucose (1 g/kg of body weight). To determine insulin sensitivity, 6-h-fasted mice were intraperitoneally administered with insulin (1 U/kg of body weight). Blood glucose from tail-vein blood was quantified by a NovaMax glucometer at designated time after administration.

2.4. Cell lines

Brown preadipocyte cell line derived from the stromal-vascular fraction was established and provided by Dr. Huang from Model Animal Research Center of Nanjing University. Cells were cultured in high glucose (5 mM) DMEM containing 10% fetal bovine calf serum (FBS). Immortalized brown adipocytes was induced by stimulation with 50 mM IBMX, 1 mM dexamethasone, 20 nM insulin, 125 mM indomethacin, and 1 nM T3 in full medium. After 48 h, the medium was exchanged for full medium plus 20 nM insulin and 1 nM T3. Cells were maintained in this medium until sampling for analysis. To stimulate UCP1 expression for final read-out, the cells were incubated in full medium with 1 μM isoproterenol for 12 h before fixation or lysis. The inducible medium of 3T3L1 cell differentiation was out of indomethacin, and the maintaining medium was out of T3, while the other ingredients were same. Isoproterenol (I5627, Sigma, 1 μM), recombinant mouse FSTL1 protein (1738-FN, R&D Systems, 100 ng/ml), SR59230A (S8688, Sigma, 0.1 μM) were added into culture medium when needed.

2.5. RNA Interference and lentivirus production

To knock down FSTL1 in brown preadipocytes, lentiviral vector (hU6-MCS-Ubiquitin-EGFP-IRES-puromycin) containing the short-hairpin RNA (shRNA) specifically targeting FSTL1 or a negative control sequence was constructed (GeneChem, Shanghai, China), the sequences were as follows:

Fstl1-RNAi (55013-1) NM_008047 5′-AGAATGAAACAGCCATCAA-3′
Fstl1-RNAi (55014-1) NM_008047 5′-AGGTGAACACCAAAGAGAT-3′
Fstl1-RNAi (55015-1) NM_008047 5′-CTGCATTGAGCAATGCAAA-3′
Negative control RNAi: 5′-TTCTCCGAACGTGTCACGT-3′.

Brown preadipocytes were transfected with lentiviral vector containing shRNA sequences for relevant RNA interference experiments and then subjected to differentiation. The experimental details were shown in our previously study [30]. To overexpress PPARγ2 in brown adipocytes, lentiviruses were produced by transfecting pLVX-PPARγ2 plasmids (a kind gift from Dr. Huang), pSPAX2 and pMD2G (purchased from Addgene) into 293T cells, viral particles accumulated in the supernatant and high-titer viral preparations could be obtained by ultracentrifugation, lentivirus was titrated before transfecting into brown adipocytes with polybrene.

To overexpress FSTL1 in brown adipocytes, GV141 vector (CMV-MCS-3FLAG-SV40-Neomycin) containing a FSTL1 coding sequence (NM_008047) was constructed (GeneChem, Shanghai, China). Brown adipocytes were incubated with 2 μg DNA and 6 μl lipofectamine 2000 diluted in Opti-MEM for 48 h and then subjected to differentiation. The empty vector was used as a control.

2.6. Protein extraction and western blotting

Cells and tissues were lysed in the RIPA buffer with protease inhibitor and protein phosphatase inhibitor. Membrane protein extraction was followed by instructions of Mem-PER Plus Membrane Protein Extraction Kit (89,842; Thermo scientific). Protein concentration was determined with BCA Protein assay kit (Thermo Scientific, Rockford, IL, USA), the amount of protein we sampled was 40–60 μg per lane. The primary antibodies used were Mouse FSTL1 antibody (1:2000, AF1738 R&D Systems), UCP1 (1:1000, ab10983 abcam), PPARγ (1:1000, #2443 Cell Signaling Technology), FLAG antibody (1:1000, #14793 Cell Signaling Technology), Normal Rabbit IgG (same concentration as the specific antibody, #2729 Cell Signaling Technology), β3-AR(C-5) (1:1000, sc-515,763 Santa Cruz Biotechnology), PKA C-α (1:1000, #4782 Cell Signaling Technology), GAPDH (1:3000, #5174 Cell Signaling Technology). Western blot analyses were performed following standard protocols as described previously [31].

2.7. Coimmunoprecipitation and GST pull-down assays

For coimmunoprecipitation of endogenous FSTL1 and β3-AR, 293 T cells were transfected with GV141 vector containing a FSTL1 coding sequence as mentioned above and GV417 vector (CMV-MCS-IRES-Cherry-SV40-Neomycin) containing a β3-AR coding sequence (NM_013462). The whole experimental procedure was followed by instructions (26146; Thermo scientific). For immunoprecipitation, equal aliquots of tissue lysates were incubated with anti-FLAG antibody or anti-β3-AR antibody overnight at 4 °C, normal rabbit IgG was used as control. Then tissue lysates were incubated with protein A/G-conjugated agarose beads at 4 °C for 4 h. Beads were washed with IP lysis/Wash Buffer for three times separately. Proteins were immunoblotted using antibodies as described above.

GST-fused constructs were expressed in BL21 *Escherichia coli*. In vitro transcription and translation experiments were done with rabbit reticulocyte lysate (TNT systems, Promega) according to the manufacturer's recommendation. For GST pull-down assays, about 5 mg of the appropriate GST fusion proteins with 30 ml of glutathione-Sepharose beads was incubated with 5–8 ml of in vitro transcribed/translated products in binding buffer (75 mM NaCl, 50 mM HEPES, pH 7.9) at 4 °C for 2 h in the presence of the protease inhibitor mixture. The beads were washed 5 times with binding buffer, resuspended in 30 ml of 2 × SDS-PAGE loading buffer, and detected by western blotting.

2.8. RNA extraction, cDNA synthesis, and quantitative real-time PCR

Total cellular RNA was extracted from brown adipose tissue and brown adipocytes using Trizol reagent (Thermo Fisher Scientific). RNA concentration was about 1500–3000 ng/μl determined with NanoDrop2000. Quantitative real-time reverse transcription polymerase chain reaction (qRT-PCR) analysis was performed as previously described [32]. The primer sets we used were as Table S.1. Relative mRNA levels were measured using the CFX96 Real-time System, C1000 Thermal Cycler (BioRad).

2.9. Reaction for protein deglycosylation

Reaction protocols for protein deglycosylation were followed by instructions of protein deglycosylation mix II (P6044; NEB). Dissolve 100 μg of glycoprotein into 40 μl H_2O. To the native glycoprotein add 5 μl 10× deglycosylation mix buffer 1. Add 5 μl protein deglycosylation mix II,

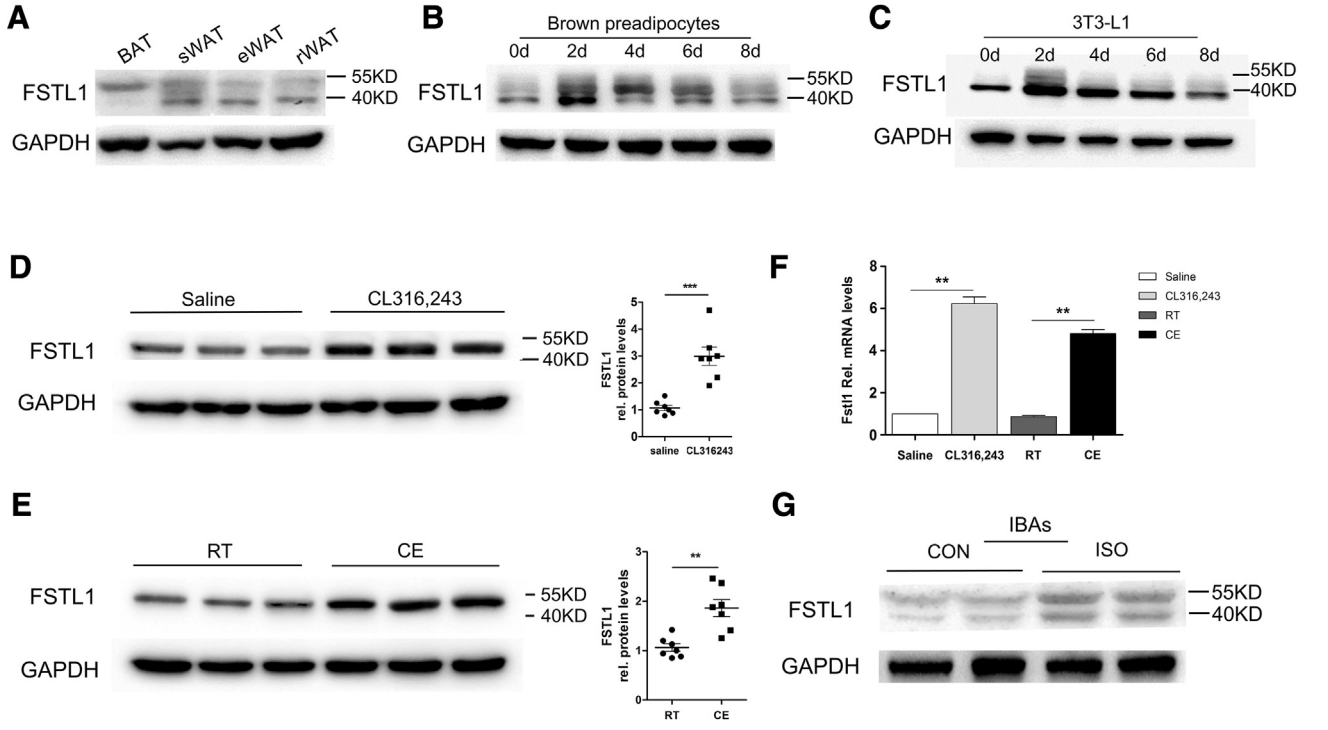

Fig. 1. FSTL1 expression in BAT was induced by β-adrenergic stimulation (A) The protein levels of FSTL1 in brown adipose tissue (BAT), subcutaneous white adipose tissue (sWAT), epididymal white adipose tissue (eWAT), retroperitoneal white adipose tissue (rWAT). 50 KD, glycosylated; 37 KD, hypoglycosylated. (B) Time course of FSTL1 expression during brown preadipocytes differentiation. (C) Time course of FSTL1 expression during 3T3L1 cell differentiation. (D) Western Blot of FSTL1 protein levels in BAT from 8-week-old male mice 4 h after saline or CL316,243 (1 mg/kg) injection (Left); densitometric quantification was calculated relative to GAPDH protein levels, all individuals involved were performed (Right). Data are Mean ± SEM, Student's *t*-test, *** $p < 0.005$, $n = 8$. (E) The protein levels of FSTL1 in BAT from 8-week-old male mice housed in cages at room temperature (24 °C) or cold exposure (4 °C) for 8 h without food and water (Left); densitometric quantification was calculated relative to GAPDH protein levels, all individuals involved were performed (Right). Data are Mean ± SEM, Student's *t*-test, ** $p < 0.01$, $n = 8$. (F) Mice were pre-treated with CL316,243 injection or cold exposure as in D and E. mRNA levels of *Fstl1* in BAT were calculated relative to β-actin mRNA levels using the ΔΔCt method. Data are Mean ± SEM, Student's *t*-test, ** $P < 0.01$, $n = 3$. (G) The protein level of FSTL1 in immortalized brown adipocytes (IBAs) with or without ISO (1 μM for 12 h) treatment.

mix gently. Incubate reaction at 25 °C (room temperature) for 30 min. Transfer reaction to 37 °C, incubate for 16 h. Proteins were immunoblotted using FSTL1 antibody to confirm the deglycosylation was effective. Brown adipocytes were incubated with supernatant, deglycosylation supernatant or Deglycosylation Mix for 12 h.

2.10. Statistical analysis

All statistical analysis was performed using SPSS software (v.20) or GraphPad Prism (v.5.0). Statistical significance was defined as $^{*}p < 0.05$, $^{**}p < 0.01$, and $^{***}p < 0.005$ and determined by two-tailed Student's *t*-tests (for comparison of two experimental conditions) or ANOVA (for comparison of three or more experimental conditions). The number of animals used for each experiment is indicated in the figure captions. For cell studies, data are representative of at least three independent experiments unless otherwise specified.

3. Results

3.1. FSTL1 expression was correlated with BAT activation

To determine the potential effect of FSTL1 on thermogenesis, we first detected the expression of FSTL1 protein in various adipose tissues of C57BL/6J mice. FSTL1 was highly expressed and glycosylated in BAT (Fig. 1A). Glycosylated, hypo-glycosylated, and non-glycosylated FSTL1 could be detected in subcutaneous WAT (sWAT), while the non-glycosylated FSTL1 was the dominant form in renal and epididymal WAT (Fig. 1A). We then differentiated brown preadipocytes and 3T3-L1 cells in culture and found that FSTL1 expression was initially upregulated after induction and then gradually reduced (Fig. 1B, C). Interestingly, glycosylated form of FSTL1 prevailed once brown preadipocytes were differentiated, while FSLT1 remained largely un-glycosylated during the differentiation of 3T3-L1 white fat cells. These data suggest that FSTL1 glycosylation is associated with the thermogenic ability of adipose tissues.

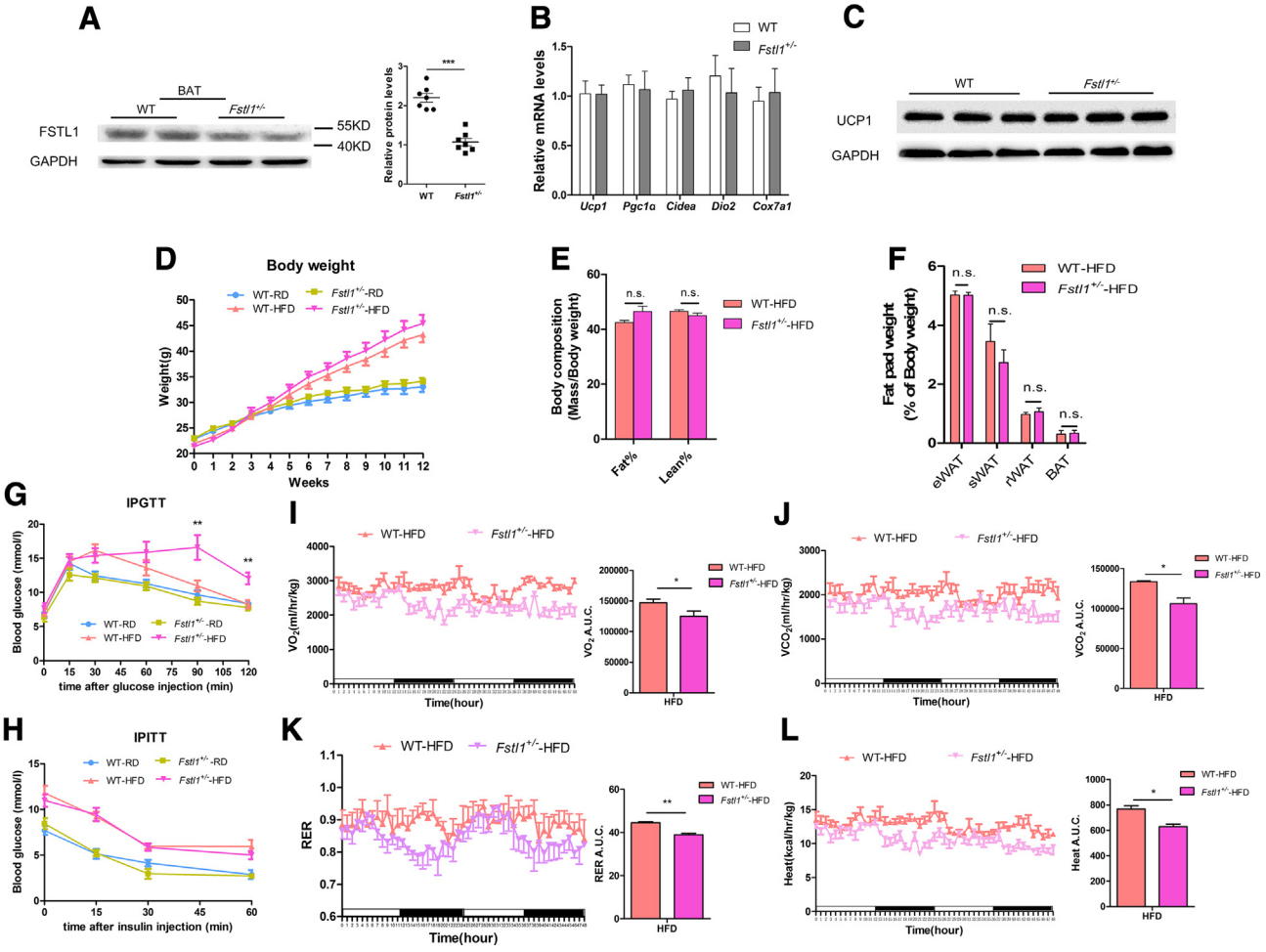

Fig. 2. FSTL1 haploinsufficiency impaired HFD-induced energy expenditure and developed glucose intolerance. (A)Western Blot of FSTL1 protein levels in BAT from WT and *Fstl1*$^{+/-}$ mice (left); densitometric quantification was calculated relative to GAPDH protein levels, all individuals involved were performed (Right). Data are Mean ± SEM, Student's t-test, *** $p < 0.005$, n = 8. (B) Relative mRNA abundance of *UCP1, Pgc1α, Cidea, Dio2* and *Cox7a1* in BAT from WT and *Fstl1*$^{+/-}$ mice. Data are Mean ± SEM, Student's t-test, no asterisk when $P > 0.05$, n = 3. (C)Western Blot analysis of protein levels of UCP1 in BAT from WT and *Fstl1*$^{+/-}$ mice. (D)WT and *Fstl1*$^{+/-}$ mice were fed regular diet (RD) or high fat diet (HFD) for 12 weeks. Total body weight was determined weekly. Data are Mean ± SEM, Student's t-test, no asterisk when $P > 0.05$, $n = 12$. (E) Total fat mass and lean mass (normalized to body weight) of WT and *Fstl1*$^{+/-}$ mice after 12 weeks of HFD feeding. Data are Mean ± SEM, Student's t-test, no asterisk when $P > 0.05$, n = 12. (F) Fat pad weight (normalized to body weight) of WT and *Fstl1*$^{+/-}$ mice after 12 weeks of HFD feeding. Data are Mean ± SEM, Student's t-test, no asterisk when $P > 0.05$, n = 12. (G and H) Geneotype-induced effects on glucose metabolism were assessed by intra-peritoneal glucose tolerance test (IPGTT, G) and intra-peritoneal insulin tolerance test (IPITT, H) in WT and *Fstl1*$^{+/-}$ mice after 12 weeks RD or HFD feeding. Data are Mean ± SEM, Two-way ANOVA followed by Bonferroni post-tests, $^{**}P < 0.01$ for WT-HFD versus *Fstl1*$^{+/-}$-HFD in G, No asterisk when $P > 0.05$, $n = 6$. (I) O_2 consumption of WT and *Fstl1*$^{+/-}$ mice after 12 weeks of HFD feeding (Left); AUC analysis of VO_2 during the measurement (Right). Data are Mean ± SEM, Student's t-test $^{*}P < 0.05$, $n = 4$. (J) CO_2 production of WT and *Fstl1*$^{+/-}$ mice after 12 weeks of HFD feeding (Left); AUC analysis of VCO_2 during the measurement (Right). Data are Mean ± SEM, Student's t-test *P < 0.05, n = 4. (K) Respiratory exchange rate (RER) of WT and *Fstl1*$^{+/-}$ mice after 12 weeks of HFD feeding (Left); AUC analysis of RER during the measurement (Right). Data are Mean ± SEM, Student's t-test $^{**}P < 0.01$, n = 4. (L) Heat production of WT and *Fstl1*$^{+/-}$ mice after 12 weeks of HFD feeding (Left); AUC analysis of heat production during the measurement (Right). Data are Mean ± SEM, Student's t-test *P < 0.05, n = 4.

Cold exposure (CE) and β3-adrenergic receptor agonist are the most effective ways to activate brown fat. Notably, FSTL1 expression in BAT was significantly upregulated in mice either intraperitoneally injected with CL316,243 (CL) or exposed to cold (Fig. 1D, E). *Fstl1* mRNA levels in BAT were also significantly elevated after CL316,243 injection or cold exposure (Fig. 1F). Isoproterenol (ISO), a broad β-adrenergic receptor agonist, could increase FSTL1 protein level in in-vitro differentiated, immortalized brown adipocytes (IBAs) (Fig. 1G). These results indicate that the adrenergic receptor signaling in brown adipocytes is directly involved in regulating FSTL1 expression.

3.2. FSTL1 haploinsufficiency did not impair systemic metabolism when BAT was not fully activated

We then sought to determine the biological function of FSTL1 in BAT using a loss-of-function mouse model. Heterozygous *Fstl1*$^{+/-}$ mice were used in this study (Fig. S.4A), as homozygous *Fstl1*$^{-/-}$ mice die of respiratory failure shortly after birth [33]. FSTL1 protein level in BAT of *Fstl1*$^{+/-}$ mice was approximately the half of that of *Fstl1*$^{+/+}$ wildtype (WT) mice (Fig. 2A). However, mRNA levels of thermogenic genes including *Ucp1*, *Ppargc1a*, *Cidea*, *Dio2*, and *Cox7a1* were almost equal between WT and *Fstl1*$^{+/-}$ mice (Fig. 2B). UCP1 protein was also not affected (Fig. 2C). In addition, body weight, glucose tolerance, and insulin tolerance were also comparable between WT and *Fstl1*$^{+/-}$ mice (Fig. 2D, G, H). Energy expenditure assessment showed that O_2 consumption, CO_2 production, respiratory exchange ratio (RER), and heat production were also equal between WT and *Fstl1*$^{+/-}$ mice with RD feeding (Fig. S.1A–D). These data indicate that FSTL1 is dispensable for thermogenic gene expression and systemic metabolism when brown fat is not fully activated.

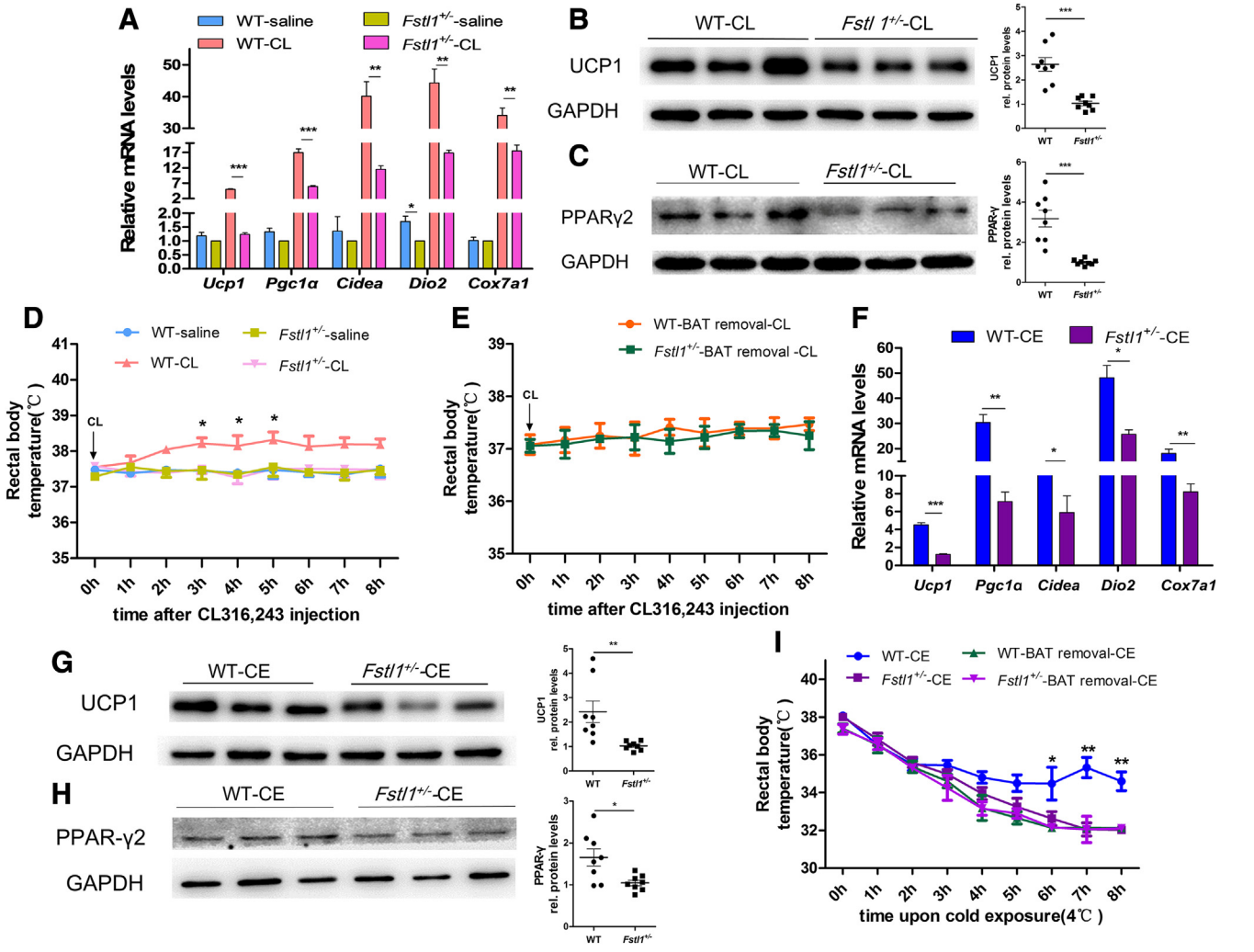

Fig. 3. FSTL1 ablation impaired adaptive thermogenesis of BAT (A) Mice were intraperitoneally (i.p.) injected with saline or CL316,243 (1 mg/kg), Real-time qPCR analysis of genes involved in thermogenesis in BAT of WT and *Fstl1*$^{+/-}$ mice 4 h after saline or CL316,243 injection. Data are Mean ± SEM, Two-way ANOVA followed by Bonferroni post-tests, *P < 0.05, **P < 0.01, ***P < 0.005, WT-CL versus *Fstl1*$^{+/-}$-CL, *n* = 3. (B and C) Western Blot of UCP1 and PPARγ2 protein levels in BAT from WT and *Fstl1*$^{+/-}$ mice 4 h after saline or CL316,243 injection (B, C Left); densitometric quantification was calculated relative to GAPDH protein levels, all individuals involved were performed (B, C Right). Data are Mean ± SEM, Student's t-test, ***P < 0.005, n = 8. (D) WT and *Fstl1*$^{+/-}$ mice were intraperitoneally (i.p.) injected with saline or CL316,243 (1 mg/kg), the rectal temperature was measured every hour for a total of 8 times. Data are Mean ± SEM, Two-way ANOVA followed by Bonferroni post-tests, *P < 0.05, WT-CL versus *Fstl1*$^{+/-}$-CL, n = 8. (E) After BAT removal operation, WT and *Fstl1*$^{+/-}$ mice were intraperitoneally (i.p.) injected with CL316,243 (1 mg/kg), the rectal temperature was measured every hour for a total of 8 times. Data are Mean ± SEM, Two-way ANOVA followed by Bonferroni post-tests, no asterisk when P > 0.05, n = 4. (F) Thermogenic gene expression in BAT of WT and *Fstl1*$^{+/-}$ mice after cold exposure for 8 h. Data are Mean ± SEM, Student's t-test, *P < 0.05, **P < 0.01, ***P < 0.005, *n* = 3. (G and H) Western Blot of UCP1 and PPARγ2 protein levels in BAT from WT and *Fstl1*$^{+/-}$ mice after cold exposure for 8 h (H, I Left); densiometric quantification was calculated relative to GAPDH protein levels, all individuals involved were performed (H, I Right). Data are Mean ± SEM, Student's t-test, *P < 0.05, **P < 0.01, n = 8. (I) Body temperature upon cold exposure for 8 h of WT and *Fstl1*$^{+/-}$ mice after BAT removal operation or not. Data are Mean ± SEM, Two-way ANOVA followed by Bonferroni post-tests, *P < 0.05, **P < 0.01, WT-CE versus *Fstl1*$^{+/-}$-CE, n = 4.

3.3. FSTL1 ablation caused imbalance of diet-induced energy expenditure and developed glucose intolerance of mice

Feeding mice a high fat diet (HFD) could slowly recruit BAT and promotes energy expenditure [34]. To better understand the role of FSTL1 in BAT, we fed WT and *Fstl1*$^{+/-}$ mice with HFD for 12 weeks. Although the body weight of *Fstl1*$^{+/-}$ mice showed a slight increasing tendency (Fig. 2D), but the WAT depots were at the same level (Fig. 2E, F). However, IPGTT indicated the presence of impaired glucose tolerance of *Fstl1*$^{+/-}$ mice after HFD feeding (Fig. 2G), while similar trends were observed in insulin tolerance test (Fig. 2H). We also assessed the rates of energy expenditure in WT and *Fstl1*$^{+/-}$ mice feeding high fat diet (HFD). After 12 weeks of HFD feeding, O_2 consumption (Fig. 2I), CO_2 production (Fig. 2J), RER (Fig. 2K), and heat production (Fig. 2L) in WT mice were at a higher lever compared to *Fstl1*$^{+/-}$ mice. UCP1 expression in BAT of WT mice was slightly higher than *Fstl1*$^{+/-}$ mice (Fig. S.2A), BAT histology showed no obvious difference (Fig. S.2B). No difference was observed in food intake, water drink, or physical activity between the two groups with HFD or RD feeding (Fig. S.1E-G). Together, these results suggest that FSTL1 plays a role in diet-induced systemic metabolism, while it is not clear how FSTL1 functions when brown fat is fully activated.

3.4. FSTL1 deficiency impaired adaptive thermogenesis when BAT is fully activated

To test whether FSTL1 has an essential regulatory role in adaptive thermogenesis, we next treated mice with either CL316,243 or cold exposure to recruit BAT. CL316,243 profoundly increased the expression of thermogenic genes in BAT, but such induction was significantly diminished in *Fstl1*$^{+/-}$ mice (Fig. 3A). After CL316,243 treatment, levels of UCP1 and PPARγ2 proteins in BAT of *Fstl1*$^{+/-}$ mice were much lower than those in WT mice (Fig. 3B, C). Moreover, CL316,243 increased core body temperature in WT mice but not *Fstl1*$^{+/-}$ mice (Fig. 3D), while this difference disappeared when interscapular BAT was removed (Fig. 3E). Similarly, *Fstl1*$^{+/-}$ mice also had reduced thermogenic gene expression (Fig. 3F), expression of UCP1 and PPARγ2 at the protein level (Fig. 3G, H), and body temperature (Fig. 3I) after cold exposure for 8 h, when compared to WT controls. Cold-induced difference of body temperature was also disappeared when BAT was removed (Fig. 3I). But during the long-term cold exposure, WT and *Fstl1*$^{+/-}$ mice exhibited considerable browning and UCP1 expression in subcutaneous white adipose tissue (sWAT) (Fig. S.2C, D). Gene expression of browning markers in sWAT were also equal between the two groups (Fig. S.2E). As expected, there was also no difference in body temperature between WT and *Fstl1*$^{+/-}$ mice during 72 h cold exposure

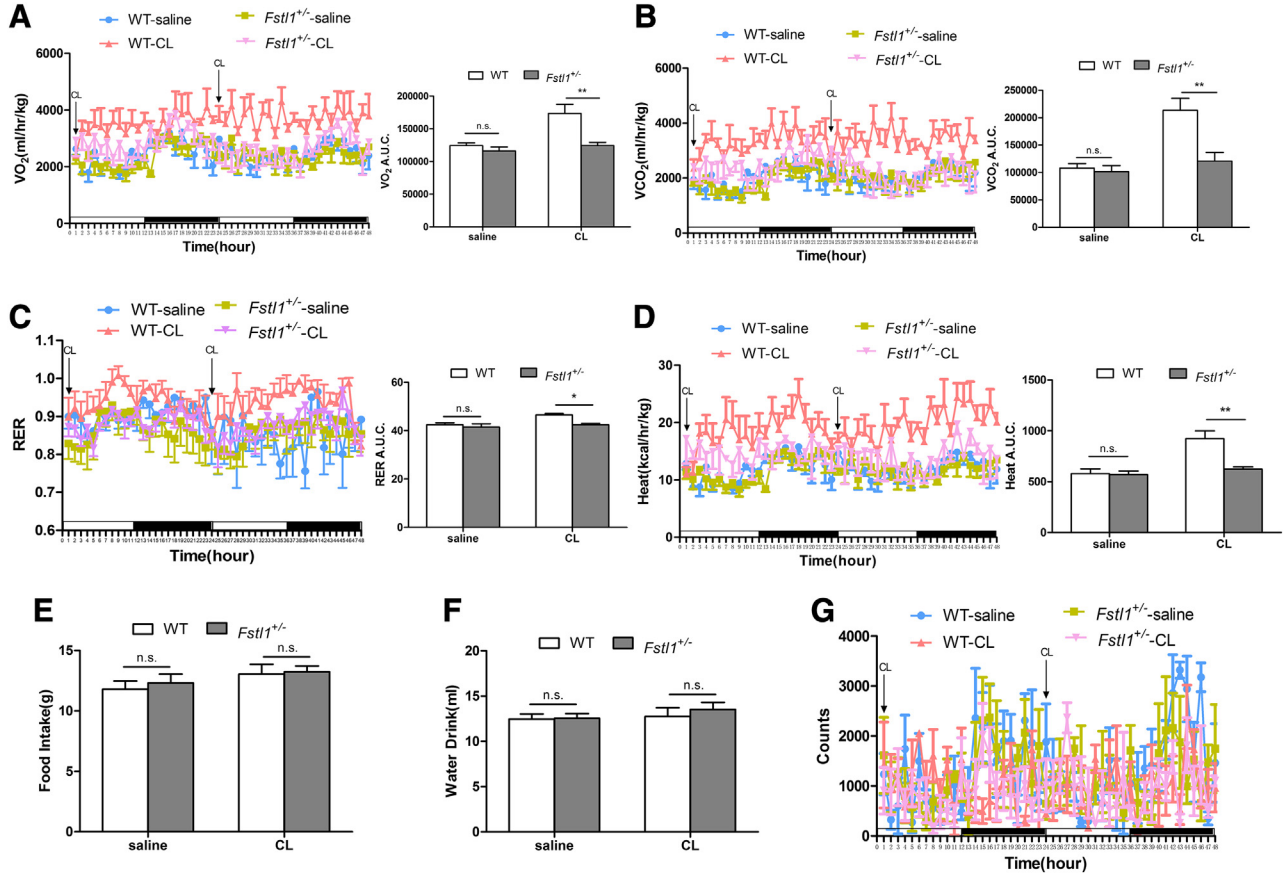

Fig. 4. FSTL1 deficiency led to a reduction in oxidative respiration of mice when stimulated by CL316,243. (A) O_2 consumption of WT and *Fstl1*$^{+/-}$ mice with saline or CL316,243 (1 mg/kg BM, i.p.) injection (Left); AUC analysis of VO_2 during the measurement (Right). Data are Mean ± SEM, Two-way ANOVA followed by Bonferroni post-tests, $^{**}P < 0.01$, WT-CL versus *Fstl1*$^{+/-}$-CL, n = 4. (B) CO_2 production of WT and *Fstl1*$^{+/-}$ mice with saline or CL316,243 (1 mg/kg BM, i.p.) injection (Left); AUC analysis of VCO_2 during the measurement (Right). Data are Mean ± SEM, Two-way ANOVA followed by Bonferroni post-tests, $^{**}P < 0.01$, WT-CL versus *Fstl1*$^{+/-}$-CL, n = 4. (C) Respiratory exchange rate (RER) of WT and *Fstl1*$^{+/-}$ mice with saline or CL316,243 (1 mg/kg BM, i.p.) injection (Left); AUC analysis of RER during the measurement (Right). Data are Mean ± SEM, Two-way ANOVA followed by Bonferroni post-tests, $^{*}P < 0.05$, WT-CL versus *Fstl1*$^{+/-}$-CL, n = 4. (D) Heat production of WT and *Fstl1*$^{+/-}$ mice with saline or CL316,243 (1 mg/kg BM, i.p.) injection (Left); AUC analysis of heat production during the measurement (Right). Data are Mean ± SEM, Two-way ANOVA followed by Bonferroni post-tests, $^{**}P < 0.01$, WT-CL versus *Fstl1*$^{+/-}$-CL, n = 4. (E and F) Total food intake (E) and water drink (F) of mice in each group during one complete 12 h light-dark cycle. Data are Mean ± SEM, Two-way ANOVA followed by Bonferroni post-tests, no asterisk when $P > 0.05$, n = 4. (G)Free activity of WT and *Fstl1*$^{+/-}$ mice with saline or CL316,243 (1 mg/kg BM, i.p.) injection.

(Fig. S.2F). These data suggest that FSTL1 is more significant during acute BAT recruitment.

Further, we subjected *Fstl1*$^{+/-}$ and littermate controls injected with CL316,243 or saline to metabolic cage analysis. As expected, O_2 consumption (Fig. 4A), CO_2 production (Fig. 4B), respiratory exchange ratio (RER, Fig. 4C), and heat production (Fig. 4D) in WT mice were augmented by CL316,243. However, *Fstl1*$^{+/-}$ mice were refractory to CL316,243-induced thermogenic activation (Fig. 4A-D). No difference in food intake, water drink, or physical activity was observed among the four groups (Fig. 4E-G). Moreover, BAT mass of WT mice were increased after CL316,243 injection but not in *Fstl1*$^{+/-}$ mice (Fig. S.4E, F). Together, these results show that FSTL1 ablation attenuated the adaptive thermogenesis induced by β3-adrenergic activation and cold exposure.

3.5. FSTL1 enhanced the β3-adrenergic signaling and thus inducing the thermogenic gene expression

FSTL1 has been demonstrated to inhibit SMAD1/5/8-mediated BMP4 signaling and SMAD2/3-mediated TGF-β1 signaling in the lung [33,35]. However, we did not observe any significant changes in levels of p-SMAD1/5/8 or p-SMAD2/3 in *Fstl1*$^{+/-}$ BAT (Fig. S.3A, B) or in vitro-differentiated brown adipocytes with FSTL1 knockdown (Fig. S.3C, D), indicating that the SMAD signaling may not mediate the effect of FSTL1 on BAT function.

Considering that FSTL1 was indispensable for CL316,243-induced thermogenesis, we then sought to determine its effect on β3-AR level. Although β3-AR protein expression in BAT only showed a slight decreasing tendency in *Fstl1*$^{+/-}$ mice housed at room temperature (Fig. S.4B), it was significantly decreased after CL316,243 injection or cold exposure (Fig. 5A, B). While the level of β3-AR protein had a significantly decrease in *Fstl1*$^{+/-}$ mice, the mRNA level remained at an equal level (Fig. S.4C).

To determine whether the regulation of β3-AR expression by FSTL1 was cell-autonomous, we first overexpressed FSTL1 in differentiated brown adipocytes in vitro. The mRNA abundance of thermogenic genes including *Ucp1*, *Cidea*, *Cox7a1*, and *Dio2* was higher in adipocytes with FSTL1 overexpression (Fig. 5C). The levels of β3-AR, PKA C-α, PPARγ2 and UCP1 proteins were also upregulated after FSTL1 overexpression (Fig. 5D). On the other hand, mRNA levels of thermogenic genes and protein levels of β3-AR, PKA C-α, PPARγ2 and UCP1 were obviously lower in isoproterenol-treated brown adipocytes when FSTL1

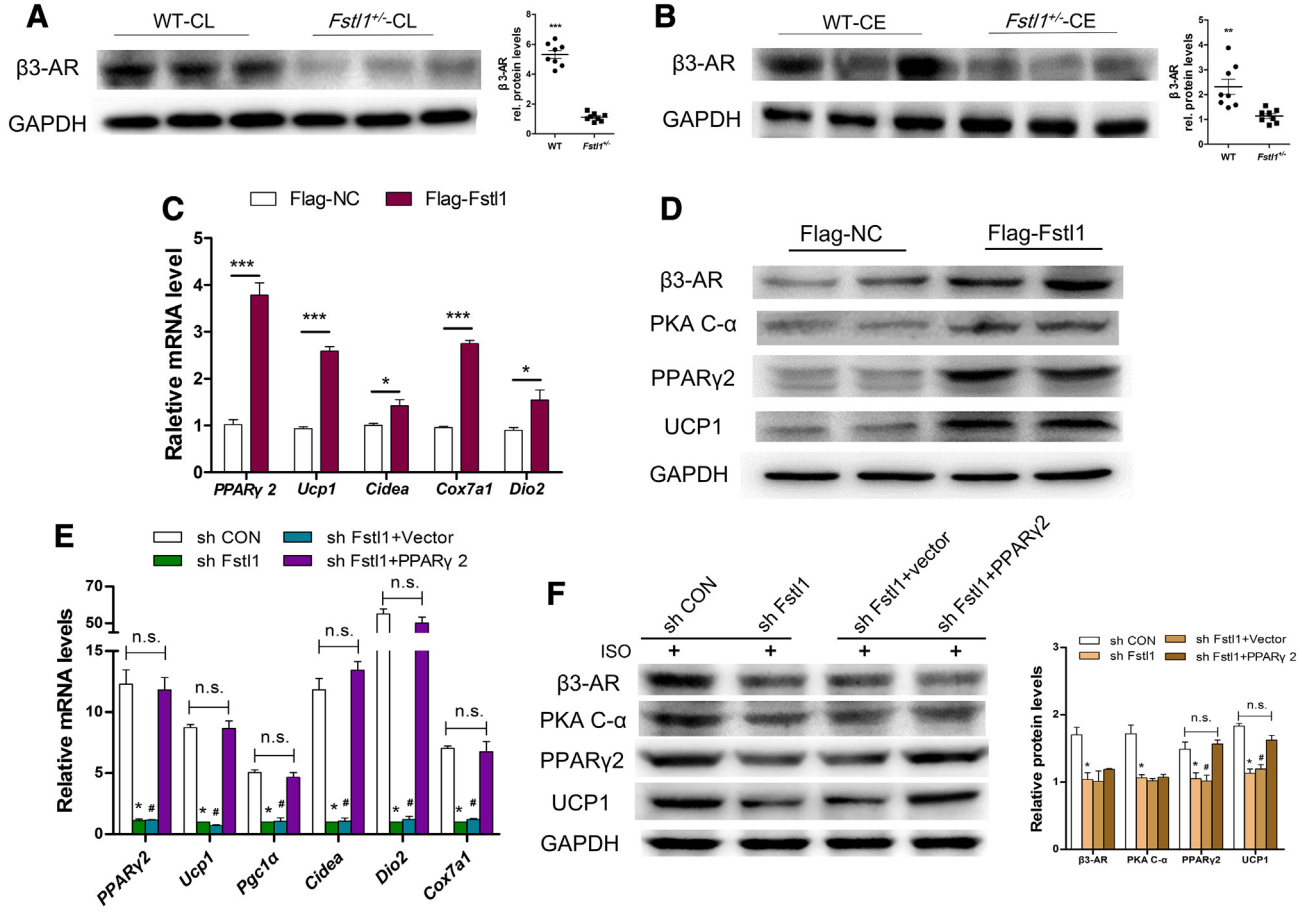

Fig. 5. FSTL1 was positively correlated with the level of β3-AR both in vivo and in vitro. (A and B) Western Blot of β3-AR protein levels in BAT from WT and *Fstl1*$^{+/-}$ mice after CL316,243 injection or cold exposure (A, B Left); densitometric quantification was calculated relative to GAPDH protein levels, all individuals involved were performed (A,B Right). Data are Mean ± SEM, Student's t-test, $^{**}P < 0.01$, $^{***}P < 0.005$, n = 8. (C) Brown preadipocytes were transfected with plasmids expressing either Flag-tagged FSTL1 (Flag-FSTL1) or negative control (Flag-NC) and then subjected to differentiation. Relative mRNA abundance of *PPARγ2, Ucp1, Cidea, Cox7a1* and *Dio2* was calculated relative to β-actin mRNA levels using the ΔΔCt method. Data are Mean ± SEM, Student's t-test, $^{*}P < 0.05$, $^{***}P < 0.005$, $n = 3$. (D) Western blot analysis of β3-AR, PKA C-α, PPARγ2 and UCP1 protein levels in brown adipocytes transfected with plasmids expressing either Flag-tagged Fstl1 (Flag-Fstl1) or negative control (Flag-NC). (E) Brown preadipocytes were separately infected with Fstl1 targeting (sh Fstl1) or non-targeting (sh CON), or co-infected with sh Fstl1 and PPARγ2 or negative control. Differentiated brown adipocytes were incubated with ISO (1 μM for 12 h). Real-time qPCR analysis of genes involved in thermogenesis (*PPARγ2, Ucp1, Pgc1α, Cidea, Cox7a1, Dio2*), mRNA levels were calculated relative to β-actin mRNA levels using the ΔΔCt method. Data are Mean ± SEM, Two-way ANOVA followed by Bonferroni post-tests, $^{*}P < 0.01$, sh CON versus sh Fstl1; $^{\#}P < 0.01$, sh Fstl1 + Vector versus sh Fstl1 + PPARγ2; n.s., not significant; n = 3. (F) Western blot analysis of β3-AR, PKA C-α, PPARγ2 and UCP1 protein levels in ISO-treated brown adipocytes infected with sh Fstl1 or sh CON, or co-infected with sh Fstl1 and PPARγ2 or negative control as mentioned above (Left); densitometric quantification was calculated relative to GAPDH protein levels (Right). Data are Mean ± SEM, Two-way ANOVA followed by Bonferroni post-tests, $^{*}P < 0.05$, sh CON versus sh Fstl1; $^{\#}P < 0.05$, sh Fstl1 + Vector versus sh Fstl1 + PPARγ2; n.s., not significant; n = 3.

was knocked down using shRNA, we further overexpressed PPARγ2 in the FSTL1 knockdown cell line, mRNA levels of thermogenic genes and UCP1 protein levels returned to equal as control group (Fig. 5E, F). These data demonstrate that the effect of FSTL1 ablation on thermogenic genes expression is achieved by regulating the expression level of PPARγ2 through β3-adrenergic signaling.

In addition, supplementing recombinant mouse FSTL1 (rFSTL1) into cultured brown adipocytes increased levels of β3-AR protein in a dose-dependent manner (Fig. 6A), this was further confirmed by β3-AR immunofluorescence staining in IBAs when rFstl1 was supplemented at 100 ng/ml (Fig. S.5). Both endogenous and exogenous FSTL1 could promote the protein levels of β3-AR, while the mRNA levels of β3-AR were not changed (Fig. S.4C, D). We then detected both mRNA and protein levels of β3-AR in brown adipocytes after incubation with rFSTL1 at different time points. It showed that mRNA levels (Fig. 6B) increased in the first hours of rFSTL1 treatment precede protein change (Fig. 6C). Furthermore, rFSTL1 and isoproterenol could additively promote the expression of β3-AR, PKA C-α, PPARγ2 and UCP1 proteins (Fig. 6D). More importantly, SR59230A, a β3-adrenoceptor antagonist, blocked the induction of PKA C-α, PPARγ2 and UCP1 expression by rFSTL1 and or isoproterenol (Fig. 6E). To find out whether there is an interaction between FSTL1 and β3-AR, binding experiments confirmed that FSTL1 directly binds β3-AR by co-IP and GST pull-down (Fig. 6F, G). Taken together, these studies indicate that the effect of FSTL1 on BAT thermogenesis is mediated by enhancing the β3-adrenergic signaling.

3.6. Glycosylation was essential for the biological function of FSTL1

The biological function of FSTL1 is closely related to its post-translational modification by N-linked glycosylation [36,37]. Consistent with the enrichment of the glycosylated FSTL1 in BAT (Fig. 1), we found the cytoplasmic FSTL1 in brown adipocytes was largely un-glycosylated while secreted FSTL1 in the medium was fully glycosylated, similar to the rFSTL1 derived from mouse melanoma cells (Fig. 7A). To determine glycosylation is functionally important, we treated conditioned medium harvested from differentiated brown adipocytes with deglycosylation enzymes. Western blotting showed that the glycosylation on FSTL1 could be fully removed by the enzyme mix (Fig. 7B). We then treated brown adipocytes with conditioned media and found that the deglycosylated medium failed to induce the expression of thermogenic genes

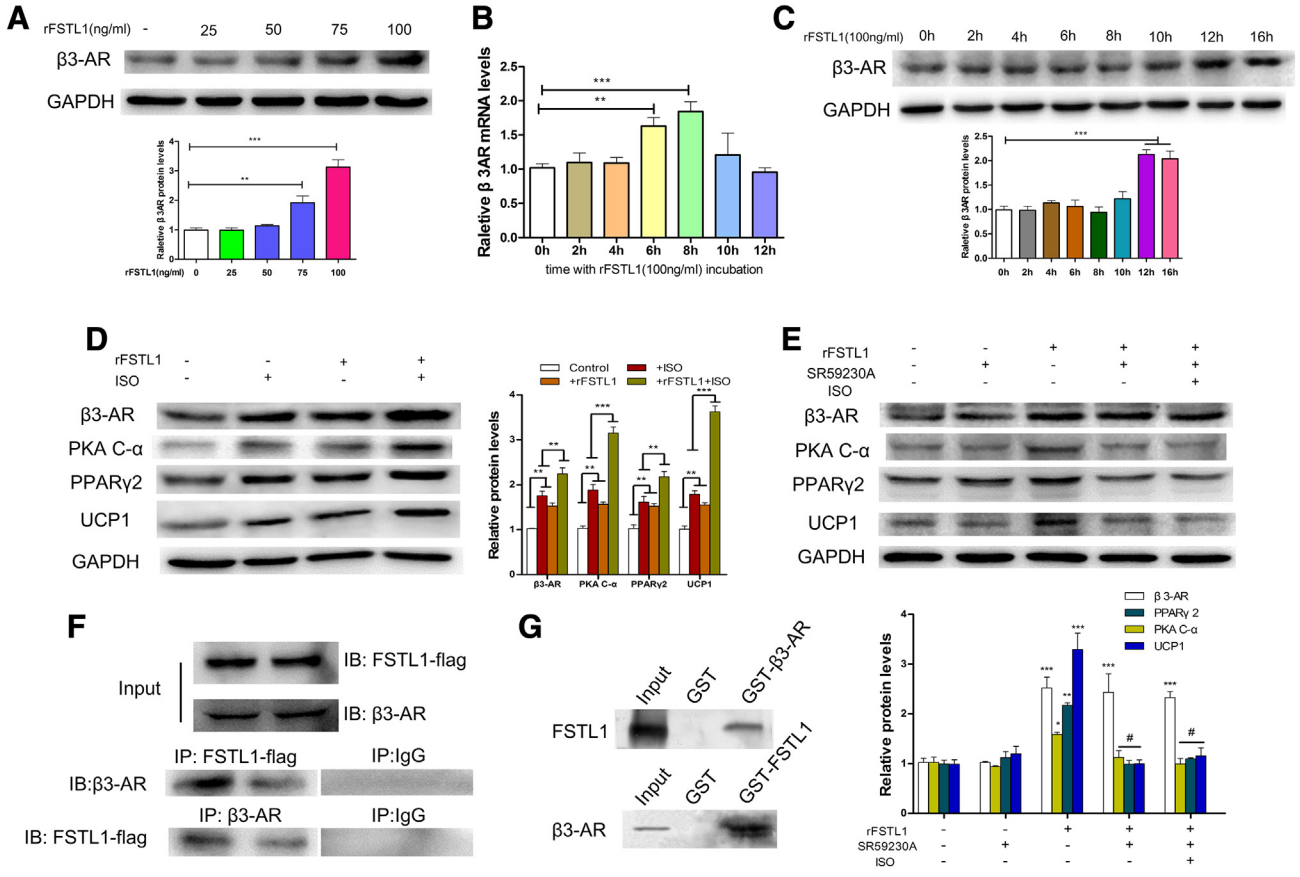

Fig. 6. FSTL1 interacted with β3-AR and thus enhancing the downstream signaling. (A) Immunoblot of β3-AR from brown adipocytes with different concentrations of recombinant mouse FSTL1 protein treated (0, 25, 50, 75, 100 ng/ml, incubation for 12 h, Upper panel); densitometric quantification was calculated relative to GAPDH protein levels (Lower panel). Data are Mean ± SEM, One-way ANOVA followed by Dunnett's multiple comparison test, $^{**}P < 0.01$, $^{***}P < 0.005$, n = 4. (B) Relative mRNA abundance of β3-AR in brown adipocytes with rFSTL1 (100 ng/ml) incubation at different time points. mRNA levels were calculated relative to β-actin mRNA levels using the ΔΔCt method. Data are Mean ± SEM, One-way ANOVA followed by Dunnett's multiple comparison test, $^{**}P < 0.01$, $^{***}P < 0.005$, n = 3. (C) Western blot analysis of β3-AR protein levels in brown adipocytes with rFSTL1 protein incubation at different time points (100 ng/ml, incubation for 0–16 h, Upper panel); densitometric quantification was calculated relative to GAPDH protein levels (Lower panel). Data are Mean ± SEM, One-way ANOVA followed by Dunnett's multiple comparison test, $^{***}P < 0.005$, n = 3. (D) The protein levels of β3-AR, PKA C-α, PPARγ2 and UCP1 in brown adipocytes treated with rFSTL1 (100 ng/ml for 12 h) or ISO (1 μM for 12 h) respectively, or both (Left); densitometric quantification was calculated relative to GAPDH protein levels (Right). Data are Mean ± SEM, Two-way ANOVA followed by Bonferroni post-tests, $^{**}P < 0.01$, $^{***}P < 0.005$, n = 3. (E) Western blot analysis of β3-AR, PKA C-α, PPARγ2 and UCP1 in brown adipocytes treated with rFSTL1 or SR59230A (0.1 μM for 1 h) respectively, or both, or rFSTL1, SR59230A and ISO, control group were incubated without any additives (upper panel); densitometric quantification was calculated relative to GAPDH protein levels (lower panel). Data are Mean ± SEM, Two-way ANOVA followed by Bonferroni post-tests, $^{*}P < 0.05$, $^{**}P < 0.01$, $^{***}P < 0.005$, $^{\#}$ for not significant, compared with control group (without any additives), n = 3. (F) 293 T cells were transfected with plasmids expressing Flag-tagged Fstl1 and β3-AR. Total cell lysate were subjected to CoIP with anti-Flag or β3-AR antibodies and immunoblotted for FSTL1 and β3-AR. Unspecific IgG antibodies were used as a control. (G) Flag-tagged Fstl1 and β3-AR protein complex was pulled down using glutathione-Sepharose beads and then subjected to Western blot analyses with anti-FSTL1 antibody to confirm the presence of FSTL1 (upper). The presence of β3-AR was detected with anti-β3-AR antibody (lower).

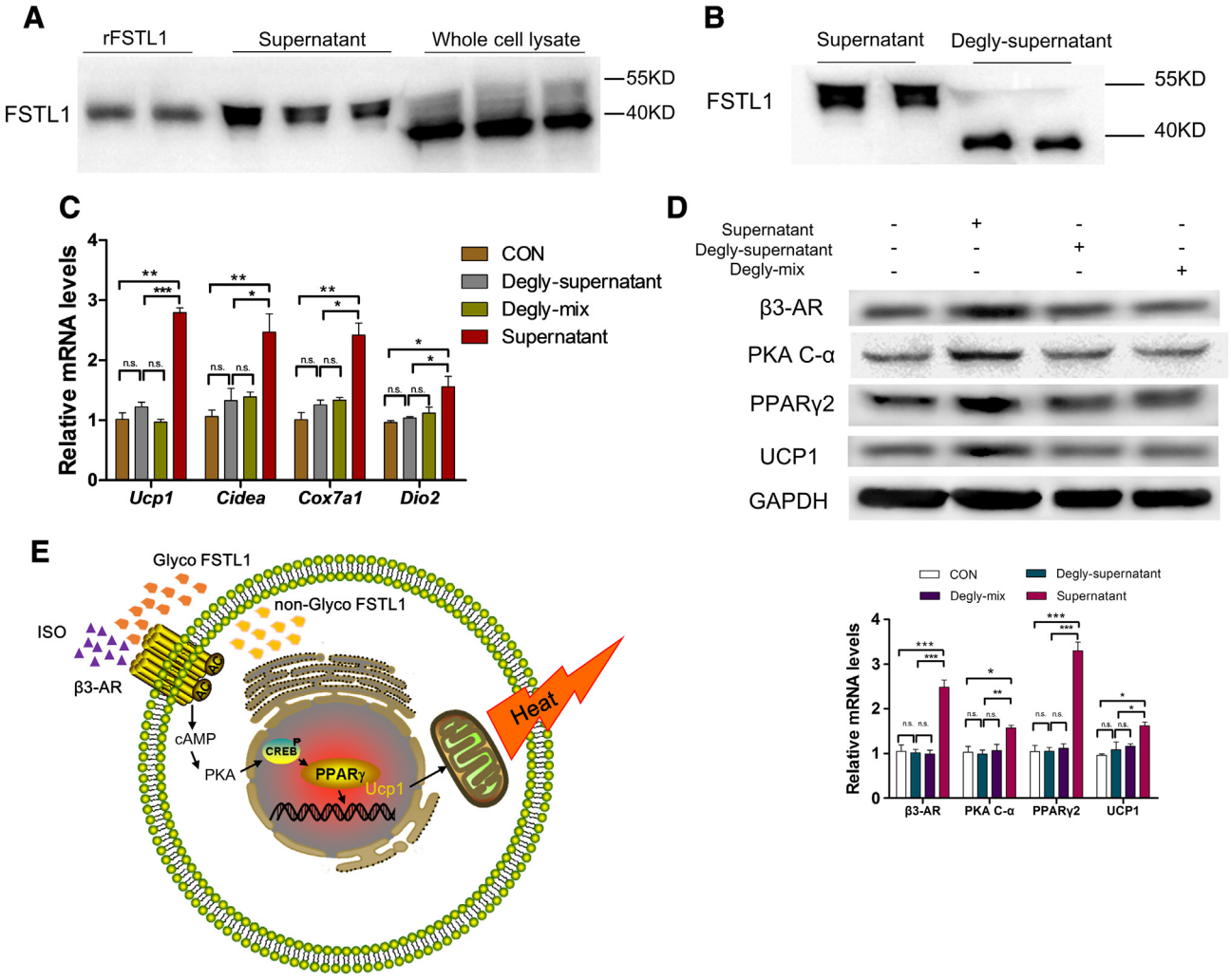

Fig. 7. Glycosylation was indispensable for the biological activity of FSTL1. (A) Immunoblot of FSTL1 in brown adipocytes lysate, culture supernatant, recombinant mouse FSTL1 protein. (B) Immunoblot of FSTL1 in brown adipocytes culture supernatant and supernatant reacting with deglycosylation enzyme. (C) Real-time qPCR analysis of mRNA levels of genes involved in thermogenesis (*Ucp1, Cidea, Cox7a1, Dio2*), brown adipocytes were treated with supernatant, deglycosylated supertanant (Degly-supernatant) or Deglycosylation Mix (Degly-mix). mRNA levels were calculated relative to β-actin mRNA levels using the ΔΔCt method. Data are Mean ± SEM, Two-way ANOVA followed by Bonferroni post-tests, $^{*}P < 0.05$, $^{**}P < 0.01$, $^{***}P < 0.005$, n = 3. (D) Western blot analysis of β3-AR, PKA C-α, PPARγ2 and UCP1 protein levels in brown adipocytes treated with supernatant, Degly-supernatant or Degly-mix as mentioned above. (Upper panel); densiometric quantification was calculated relative to GAPDH protein levels (Lower panel). Data are Mean ± SEM, Two-way ANOVA followed by Bonferroni post-tests, $^{*}P < 0.05$, $^{**}P < 0.01$, $^{***}P < 0.005$. The experiments were performed three times. (E) Summary of the role of FSTL1 in brown fat thermogenesis. Glycosylated FSTL1 enhances β3-AR-induced thermogenic gene program.

(Fig. 7C) and β3-AR, PKA C-α, PPARγ2 and UCP1 proteins (Fig. 7D). Collectively, these data demonstrate that glycosylated FSTL1 promotes the thermogenic program in BAT via the β3-adrenergic signaling (Fig. 7E).

4. Discussion

In our study, we show that the glycoprotein FSTL1 is induced by cold and β3-AR agonist and is necessary to promote BAT thermogenesis in vivo and in vitro. *Fstl1*$^{+/-}$ mice showed severe functional deficiency in BAT thermogenesis especially when they were under extreme cold exposure or injected with CL316,243, suggesting that FSTL1 is indispensable for the maximum thermogenic capacity elicited by the β3-adrenergic activation. During the in vitro adipogenic differentiation, we observed a transient upregulation of FSTL1 in both brown and white preadipocytes, indicating that FSTL1 may play a role in adipogenesis. The serum level of FSTL1 has been shown to be increased in obese patients and mice [28]. Unfortunately, our *Fstl1*$^{+/-}$ mice did not show abnormality in diet-induced obesity, which indicates that FSTL1 haploinsufficiency may not affect the differentiation and maturation of fat. However, it is still unclear whether FSTL1 is a determinant of WAT expansion in obesity or a compensatory factor for BAT activation in response to positive energy balance. BAT removal operation could exclude the effect of other tissues on thermogenesis to some extent. Future investigations on animal models that modulate FSTL1 levels in a tissue-specific manner are needed.

In WAT and BAT, FSTL1 may engage different downstream mechanisms. FSTL1 has long been proposed as an antagonist of BMP4 and an agonist of TGF-β1 signaling [33,35], and increased p-SMAD2/3 could be observed in 3 T3-L1 white adipocytes when FSTL1 was knocked down (Fig. S.6A). However, we did not detect any changes in p-SMAD2/3 or p-SMAD1/5/8 levels in BAT of *Fstl1*$^{+/-}$ mice. While BMP4 is critical for the commitment of mesenchymal stem cells into the adipogenic lineage, a recent study demonstrated that BMP4 induces the differentiation of brown preadipocytes into white-like adipocytes via the SMAD-dependent signaling [38]. Thus, it is unlikely that FSTL1 antagonizes BMP4 to promote adaptive thermogenesis. BMP7, another member of the BMP family, promotes brown adipocyte differentiation and thermogenesis via the p38 MAPK-dependent pathway [39]. It will be of interest to determine the potential interplay between FSTL1 and BMP7 in BAT thermogenesis in future experiments.

Beta-adrenergic receptors are critical for fat metabolism and weight loss [40,41]. In our study, we found that FSTL1 could promote BAT thermogenesis by enhancing the β-adrenergic signaling. In a series of overexpression and knockdown experiments, the protein levels of FSTL1 were positively correlated with levels of β3-AR, PKA C-α, PPARγ and UCP1. Although we preliminarily found the interaction between FSTL1 and β3-AR, we will further study on the structural interaction between the two proteins. Similarly to other GPCRs, the β3-AR contain seven transmembrane domains of about 22–28 residues involved in ligand binding with an intracellular C-terminus and extracellular N-terminus, the relationship between FSTL1 and C-terminus is also to be considered [42]. Moreover, the binding of FSTL1 to the DIP2A, TLR4 and BMP receptors have been shown [43,44]. It will also be interesting to determine if DIP2A, TLR4 and BMP receptor signaling pathways are involved in the action of FSTL1 in promoting the β3-adrenergic signaling.

PPARγ, particular the PPARγ2 isoform, is a key regulatory factor for brown adipocyte differentiation and BAT function [7,45]. In addition, Sirt1-dependent deacetylation of PPARγ and CDK inhibitor-induced dephosphorylation at S273 of PPARγ are important in browning of WAT [46]. Here, we find that the effect of FSTL1 in maintaining BAT thermogenesis is associated with its impact on regulating PPARγ protein expression. The efficacy of thiazolidinediones (TZDs), synthetic ligands of PPARγ in controlling blood glucose has been widely recognized [47]. However, their clinical usage is limited due to side effects including weight gain, fluid retention, bone fracture, cardiovascular disease, and bladder cancer [48–50]. Our data demonstrate PPARγ2 as a potential downstream target of FSTL1, and future experiments are required to determine the mechanisms of FSTL1 regulation of PPARγ expression.

The glycosylation state of FSTL1 is a determinant of its biological activity. For example, in cardiomyocytes the glycosylated form of FSLT1 promotes cell proliferation while the non-glycosylated FSLT1 is anti-apoptotic [37,51]. A recent study demonstrated that a single glycosylation site (N180) was sufficient and necessary to increase the proliferation of cardiomyocytes. In mouse FSTL1, three potential sites for N-glycosylation and two for O-glycosylation are present. An in vitro study has shown that only the three aspartate residues Asp^{142}, Asp^{173}, and Asp^{178} are N-glycosylated and show cell-type specificity [36]. In our study, we found that FSTL1 in brown fat cells is highly glycosylated. In contrast, FSTL1 in WAT depots are largely un- or under-glycosylated. Only the glycosylated FSTL1 can be secreted and promote the function of brown fat. It is unclear if any particular N-glycosylation sites are involved in the thermogenesis of BAT and why glycosylation is critical for the biological activity of FSTL1.

Together, our study reveals that the glycosylated FSTL1 secreted by brown fat cells promotes the thermogenic program in BAT via the β3-adrenergic signaling. Thermogenic brown and beige adipocytes provide an opportunity for developing new therapeutics for obesity and related metabolic diseases [52,53]. FSTL1 could be used to synergize with canonical β3-adrenergic agonists to activate brown fat in the future.

Funding

The present study was supported by National Natural Science Foundation of China (grant no. 81602532); Beijing Municipal Organization Department Talents Project (grant no. 2015000020124G113); Support Project of High-level Teachers in Beijing Municipal Universities in the Period of 13th Five - year Plan (grant no. IDHT20170516).

Author contributions

Y.G. and D.L.F. conceived the project and designed research. D.L.F. performed the experiments. X.Y.S. and T.L. performed tissue processing and assistance. D.L.F. and Y.G. analyzed the data and wrote the original draft. H.B.R. provided counseling on brown fat physiology and data interpretation and contributed to drafting and final editing of the manuscript.

Acknowledgements

We thank Dr. Huang from Model Animal Research Center of Nanjing University for providing us brown preadipocyte cell line derived from the stromal-vascular fraction. We thank Jingyi Zhang for providing help in English writing and Xiaowei Jia for operating on the mice. We thank Lin Shan for providing help with our experiment.

Declaration of Competing Interest

The authors declare no conflicts of interest.

References

[1] Chooi YC, Ding C, Magkos F. The epidemiology of obesity. Metabolism 2019;92:6–10. https://doi.org/10.1016/j.metabol.2018.09.005.
[2] Betz MJ, Enerbäck S. Targeting thermogenesis in brown fat and muscle to treat obesity and metabolic disease. Nat Rev Endocrinol 2017;14:77–87. https://doi.org/10.1038/nrendo.2017.132.
[3] Harms M, Seale P. Brown and beige fat: development, function and therapeutic potential. Nat Med 2013;19:1252–63. https://doi.org/10.1038/nm.3361.
[4] Chen Y, Zeng X, Huang X, Serag S, Woolf CJ, Spiegelman BM. Crosstalk between KCNK3-mediated ion current and adrenergic signaling regulates adipose thermogenesis and obesity. Cell 2017;171:836–48. https://doi.org/10.1016/j.cell.2017.09.015.
[5] Chouchani ET, Kazak L, Spiegelman BM. New advances in adaptive thermogenesis: UCP1 and beyond. Cell Metab 2019:1–11. https://doi.org/10.1016/j.cmet.2018.11.002 (January 8).
[6] Cannon B, Nedergaard J. What ignites UCP1? Cell Metab 2017;26:697–8. https://doi.org/10.1016/j.cmet.2017.10.012.
[7] Lasar D, Rosenwald M, Kiehlmann E, Balaz M, Tall B, Opitz L, et al. Peroxisome proliferator activated receptor gamma controls mature Brown adipocyte Inducibility through glycerol kinase. Cell Rep 2018;22:760–73. https://doi.org/10.1016/j.celrep.2017.12.067.
[8] Bian F, Ma X, Villivalam SD, You D, Choy LR, Paladugu A, et al. TET2 facilitates PPARγ agonist–mediated gene regulation and insulin sensitization in adipocytes. Metabolism 2018;89:39–47. https://doi.org/10.1016/j.metabol.2018.08.006.
[9] Blanchard P, Moreira RJ, Castro É, Caron A, Côté M, Andrade ML, et al. PPARγ is a major regulator of branched-chain amino acid blood levels and catabolism in white and brown adipose tissues. Metabolism 2018;89:27–38. https://doi.org/10.1016/j.metabol.2018.09.007.
[10] Chandra V, Huang P, Hamuro Y, Raghuram S, Wang Y, Burris TP, et al. Structure of the intact PPAR-γ–RXR-α nuclear receptor complex on DNA. Nature 2008;456:350–6. https://doi.org/10.1038/nature07413.
[11] Ohno H, Shinoda K, Ohyama K, Sharp LZ, Kajimura S. EHMT1 controls brown adipose cell fate and thermogenesis through the PRDM16 complex. Nature 2013;504:163–7. https://doi.org/10.1038/nature12652.
[12] Yao L, Cui X, Chen Q, Yang X, Fang F, Zhang J, et al. Cold-inducible SIRT6 regulates thermogenesis of Brown and Beige fat. Cell Rep 2017;20:641–54. https://doi.org/10.1016/j.celrep.2017.06.069.
[13] Cypess Aaron M, L S W C, Jeffrey English KCSA. Activation of human Brown adipose tissue by a b3-adrenergic receptor agonist. Cell Metablism 2015;21:33–8. https://doi.org/10.1016/j.cmet.2014.12.009.
[14] Cao W, Daniel KW, Robidoux J, Puigserver P, Medvedev AV, Bai X, et al. p38 mitogen-activated protein kinase is the central regulator of cyclic AMP-dependent transcription of the brown fat uncoupling protein 1 gene. Mol Cell Biol 2004;24:3057–67. https://doi.org/10.1128/MCB.24.7.3057-3067.2004.
[15] Rajan S, Satish S, Shankar K, Pandeti S, Varshney S, Srivastava A, et al. Aegeline inspired synthesis of novel β3-AR agonist improves insulin sensitivity in vitro and in vivo models of insulin resistance. Metabolism 2018;85:1–13. https://doi.org/10.1016/j.metabol.2018.03.001.
[16] Arch JR. Challenges in beta(3)-Adrenoceptor Agonist Drug Development. Ther Adv Endocrinol Metab 2011;2:59–64. https://doi.org/10.1177/2042018811398517.
[17] Wolff G, Taranko AE, Meln I, Weinmann J, Sijmonsma T, Lerch S, et al. Diet-dependent function of the extracellular matrix proteoglycan Lumican in obesity and glucose homeostasis. Mol Metab 2019;19:97–106. https://doi.org/10.1016/j.molmet.2018.10.007.
[18] Kong X, Yao T, Zhou P, Kazak L, Tenen D, Lyubetskaya A, et al. Brown adipose tissue controls skeletal muscle function via the secretion of Myostatin. Cell Metab 2018;28:631–43. https://doi.org/10.1016/j.cmet.2018.07.004.
[19] Sevillano J, Sánchez-Alonso MG, Zapatería B, Calderón M, Alcalá M, Limones M, et al. Pleiotrophin deletion alters glucose homeostasis, energy metabolism and brown fat thermogenic function in mice. Diabetologia 2019;62:123–35. https://doi.org/10.1007/s00125-018-4746-4.
[20] Pellegrinelli V, Peirce VJ, Howard L, Virtue S, Türei D, Senzacqua M, et al. Adipocyte-secreted BMP8b mediates adrenergic-induced remodeling of the neuro-vascular network in adipose tissue. Nat Commun 2018;9:1–18. https://doi.org/10.1038/s41467-018-07453-x.
[21] Villarroya F, Gavaldà-Navarro A, Peyrou M, Villarroya J, Giralt M. The lives and times of Brown Adipokines. Trends in Endocrinology & Metabolism 2017;28:855–67. https://doi.org/10.1016/j.tem.2017.10.005.

[22] Braga M, Reddy ST, Vergnes L, Pervin S, Grijalva V, Stout D, et al. Follistatin promotes adipocyte differentiation, browning, and energy metabolism. J Lipid Res 2014;55:375–84. https://doi.org/10.1194/jlr.M039719.
[23] Pervin S, Singh V, Tucker A, Collazo J, Singh R. Modulation of transforming growth factor-β/follistatin signaling and white adipose browning: therapeutic implications for obesity related disorders. Horm Mol Biol Clin Invest 2017;31. https://doi.org/10.1515/hmbci-2017-0036 p.
[24] An ZWIJSENHBWV, Jos AVDV. RAYMACKERS. Characterization of a rat C, glioma-secreted follistatin-related protein (FRP). Eur J Biochem 1994;225:937–46. https://doi.org/10.1111/j.1432-1033.1994.0937b.x.
[25] Hambrock HO, Kaufmann B, Müller S, Hanisch F, Nose K, Paulsson M, et al. Structural characterization of TSC-36/Flik. J Biol Chem 2004;279:11727–35. https://doi.org/10.1074/jbc.M309318200.
[26] Mattiotti A, Prakash S, Barnett P, van den Hoff MJB. Follistatin-like 1 in development and human diseases. Cell Mol Life Sci 2018;75:2339–54. https://doi.org/10.1007/s00018-018-2805-0.
[27] Wu Y, Zhou S, Smas CM. Downregulated expression of the secreted glycoprotein follistatin-like 1 (Fstl1) is a robust hallmark of preadipocyte to adipocyte conversion. Mech Develop 2010;127:183–202. https://doi.org/10.1016/j.mod.2009.12.003.
[28] Fan N, Sun H, Wang Y, Wang Y, Zhang L, Xia Z, et al. Follistatin-like 1: a potential mediator of inflammation in obesity. Mediators Inflamm 2013;2013:1–12. https://doi.org/10.1155/2013/752519.
[29] Zhang Y, X Xu, Yang Y, Ma J, Wang L, Meng X, et al. Deficiency of Follistatin-like protein 1 accelerates the growth of breast Cancer cells at lung metastatic sites. J Breast Cancer 2018;21:267–76. https://doi.org/10.4048/jbc.2018.21.e43.
[30] An J, Wang L, Zhao Y, Hao Q, Zhang Y, Zhang J, et al. Effects of FSTL1 on cell proliferation in breast cancer cell line MDA-MB-231 and its brain metastatic variant MDA-MB-231-BR. Oncol Rep 2017;38:3001–10. https://doi.org/10.3892/or.2017.6004.
[31] Meng X, Zheng R, Zhang Y, Qiao M, Liu L, Jing P, et al. An activated sympathetic nervous system affects white adipocyte differentiation and lipolysis in a rat model of Parkinson's disease. J Neurosci Res 2015;93:350–60. https://doi.org/10.1002/jnr.23488.
[32] Wang W, Meng X, Yang C, Fang D, Wang X, An J, et al. Brown adipose tissue activation in a rat model of Parkinson's disease. Am J Physiol-Endoc M 2017;313:E731–6. https://doi.org/10.1152/ajpendo.00049.2017.
[33] Geng Y, Dong Y, M Yu, Zhang L, Yan X, Sun J, et al. Follistatin-like 1 (Fstl1) is a bone morphogenetic protein (BMP) 4 signaling antagonist in controlling mouse lung development. Proc Natl Acad Sci 2011;108:7058–63. https://doi.org/10.1073/pnas.1007293108.
[34] Shi SY, Zhang W, Luk CT, Sivasubramaniyam T, Brunt JJ, Schroer SA, et al. JAK2 promotes brown adipose tissue function and is required for diet- and cold-induced thermogenesis in mice. Diabetologia 2016;59:187–96. https://doi.org/10.1007/s00125-015-3786-2.
[35] Dong Y, Geng Y, Li L, Li X, Yan X, Fang Y, et al. Blocking follistatin-like 1 attenuates bleomycin-induced pulmonary fibrosis in mice. J Exp Med 2015;212:235–52. https://doi.org/10.1084/jem.20121878.
[36] Magadum A, Singh N, Kurian AA, Sharkar MTK, Chepurko E, Zangi L. Ablation of a single N-glycosylation site in human FSTL 1 induces cardiomyocyte proliferation and cardiac regeneration. Molecular Therapy - Nucleic Acids 2018;13:133–43. https://doi.org/10.1016/j.omtn.2018.08.021.
[37] Wei K, Serpooshan V, Hurtado C, Diez-Cuñado M, Zhao M, Maruyama S, et al. Epicardial FSTL1 reconstitution regenerates the adult mammalian heart. Nature 2015;525:479–85. https://doi.org/10.1038/nature15372.
[38] Modica S, Straub LG, Balaz M, Sun W, Varga L, Stefanicka P, et al. Bmp4 promotes a Brown to white-like adipocyte shift. Cell Rep 2016;16:2243–58. https://doi.org/10.1016/j.celrep.2016.07.048.
[39] Tseng Y, Kokkotou E, Schulz TJ, Huang TL, Winnay JN, Taniguchi CM, et al. New role of bone morphogenetic protein 7 in brown adipogenesis and energy expenditure. Nature 2008;454:1000–4. https://doi.org/10.1038/nature07221.
[40] Douris N, Desai BN, Fisher FM, Cisu T, Fowler AJ, Zarebidaki E, et al. Beta-adrenergic receptors are critical for weight loss but not for other metabolic adaptations to the consumption of a ketogenic diet in male mice. Mol Metab 2017;6:854–62. https://doi.org/10.1016/j.molmet.2017.05.017.
[41] Hong S, Song W, Zushin PH, Liu B, Jedrychowski MP, Mina AI, et al. Phosphorylation of Beta-3 adrenergic receptor at serine 247 by ERK MAP kinase drives lipolysis in obese adipocytes. Mol Metab 2018;12:25–38. https://doi.org/10.1016/j.molmet.2018.03.012.
[42] Heine M, Fischer AW, Schlein C, Jung C, Straub LG, Gottschling K, et al. Lipolysis triggers a systemic insulin response essential for efficient energy replenishment of activated Brown adipose tissue in mice. Cell Metab 2018;28:644–55. https://doi.org/10.1016/j.cmet.2018.06.020.
[43] Ouchi N, Asaumi Y, Ohashi K, Higuchi A, Sono-Romanelli S, Oshima Y, et al. DIP2A functions as a FSTL1 receptor. J Biol Chem 2010;285:7127–34. https://doi.org/10.1074/jbc.M109.069468.
[44] Murakami K, Tanaka M, Usui T, Kawabata D, Shiomi A, Iguchi-Hashimoto M, et al. Follistatin-related protein/follistatin-like 1 evokes an innate immune response via CD14 and toll-like receptor 4. FEBS Lett 2012;586:319–24. https://doi.org/10.1016/j.febslet.2012.01.010.
[45] Virtue S, Petkevicius K, Moreno-Navarrete JM, Jenkins B, Hart D, Dale M, et al. Peroxisome proliferator-activated receptor γ2 controls the rate of adipose tissue lipid storage and determines metabolic flexibility. Cell Rep 2018;24:2005–12. https://doi.org/10.1016/j.celrep.2018.07.063.
[46] Li Qiang LWNK. Brown remodeling of white adipose tissue by SirT1-dependent deacetylation of Pparg. Cell 2012;150:620–32. https://doi.org/10.1016/j.cell.2012.06.027.
[47] Wagner R, Hieronimus A, Lamprinou A, Heni M, Hatziagelaki E, Ullrich S, et al. Peroxisome proliferator-activated receptor gamma (PPARG) modulates free fatty acid receptor 1 (FFAR1) dependent insulin secretion in humans. Mol Metab 2014;3:676–80. https://doi.org/10.1016/j.molmet.2014.07.001.
[48] Sun-Sil Choi EKJJ, Soo Youn YRYH, Choi HMKI Jiyoung Park, Pann-Ghill Suh PRGA. PPARg antagonist Gleevec improves insulin sensitivity and promotes the Browning of white adipose tissue. Diabetes 2016:829–39. https://doi.org/10.2337/db15-1382.
[49] Ferwana M, Firwana B, Hasan R, Al-Mallah MH, Kim S, Montori VM, et al. Pioglitazone and risk of bladder cancer: a meta-analysis of controlled studies. Diabetic Med 2013;30:1026–32. https://doi.org/10.1111/dme.12144.
[50] Emami-Riedmaier A, Schaeffeler E, Nies AT, Mörike K, Schwab M. Stratified medicine for the use of antidiabetic medication in treatment of type II diabetes and cancer: where do we go from here? J Intern Med 2015;277:235–47. https://doi.org/10.1111/joim.12330.
[51] Ogura Y, Ouchi N, Ohashi K, Shibata R, Kataoka Y, Kambara T, et al. Therapeutic impact of Follistatin-like 1 on myocardial ischemic injury in preclinical models. Circulation 2012;126:1728–38. https://doi.org/10.1161/CIRCULATIONAHA.112.115089.
[52] Mottillo EP, Desjardins EM, Crane JD, Smith BK, Green AE, Ducommun S, et al. Lack of adipocyte AMPK exacerbates insulin resistance and hepatic steatosis through Brown and Beige adipose tissue function. Cell Metab 2016;24:118–29. https://doi.org/10.1016/j.cmet.2016.06.006.
[53] Heine M, Fischer AW, Schlein C, Jung C, Straub LG, Gottschling K, et al. Lipolysis triggers a systemic insulin response essential for efficient energy replenishment of activated Brown adipose tissue in mice. Cell Metab 2018;28:644–55. https://doi.org/10.1016/j.cmet.2018.06.020.